

AD-A055 194

AIR FORCE INST OF TECH WRIGHT-PATTERSON AFB OHIO SCH--ETC F/G 17/2.1  
PERFORMANCE ANALYSIS OF CONTINUOUS-PHASE FREQUENCY SHIFT KEYING--ETC(U)  
DEC 77 K R OLSON

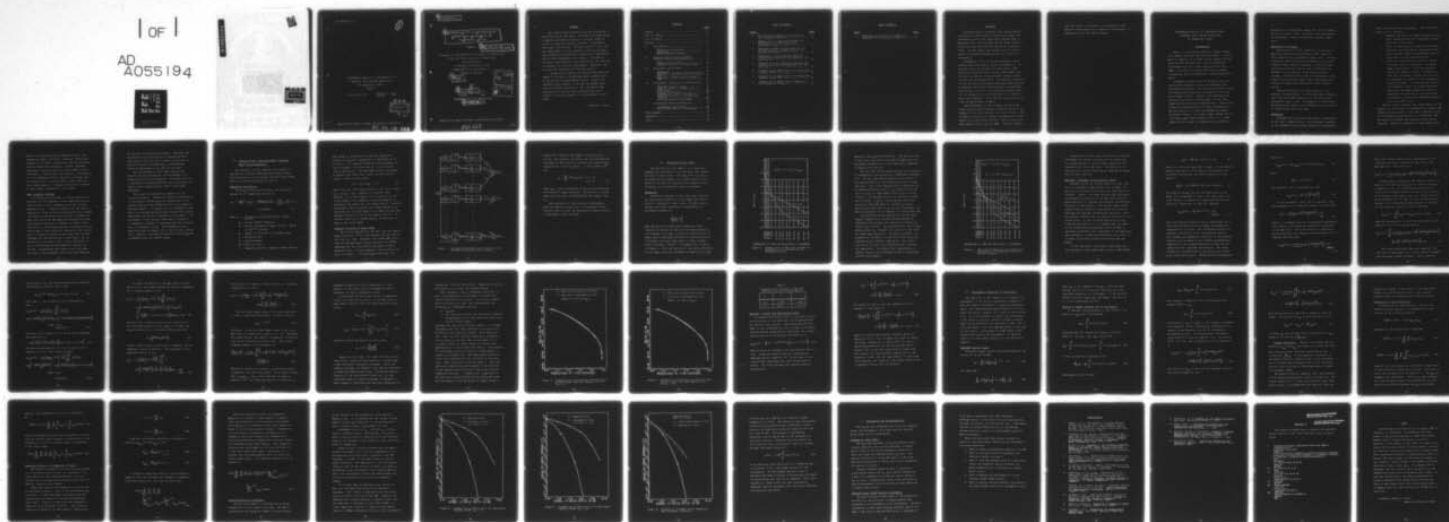
UNCLASSIFIED

AFIT/6E/EE/77-33

NL

| OF |

AD  
A055194



END  
DATE  
FILMED  
7-78  
DDC

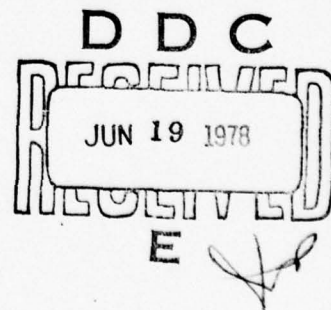
AFIT/GE/EE/77-33 ✓

①

PERFORMANCE ANALYSIS OF CONTINUOUS-PHASE  
FREQUENCY SHIFT KEYING MODULATION  
IN ATMOSPHERIC NOISE  
THESIS

AFIT/GE/EE/77-33

Kenneth R. Olson  
Captain USAF



Approved for public release; distribution unlimited

88 06 13 048

14

AFIT/GE/EE/77-33

6

PERFORMANCE ANALYSIS OF CONTINUOUS-PHASE  
FREQUENCY SHIFT KEYING MODULATION  
IN ATMOSPHERIC NOISE

THESIS

9

Master's thesis

Presented to the Faculty of the School of Engineering  
of the Air Force Institute of Technology

Air University

in Partial Fulfillment of the  
Requirements for the Degree of

Master of Science

12

56 p.

10

Kenneth H. Olson

Captain

B.S.

USAF

Graduate Electrical Engineering

11

December 1977

ACCESSION for	
NTIS	White Section <input checked="" type="checkbox"/>
DDC	Bull Section <input type="checkbox"/>
UNANNOUNCED	<input type="checkbox"/>
JUSTIFICATION	
BY	
DISTRIBUTION/AVAILABILITY CODES	
Dist.	AVAIL. and/or SPECIAL
A	

Approved for public release; distribution unlimited.

012 225

slr

## Preface

This report differs greatly from the work which I had envisioned at the onset. The plan of accomplishing a complete performance analysis of a M-ary CPFSK receiver for numerous values of M and n in atmospheric noise had to be shelved. The main reason for this was the large amount of time required to develop an amplitude probability distribution expression to approximate the Crichlow atmospheric noise model. The density function, associated with this expression, was required to evaluate the receiver performance. Therefore, the receiver was evaluated for only  $M=4$  and  $n=3$ .

I would like to express my sincere gratitude and thanks to my patient and guiding advisor, Major Carl of the Electrical Engineering faculty. Despite an extremely busy schedule of his own, he always found time for helpful discussions. The discussions and assistance provided by Capt Nejezchleb were also valuable in the development of the atmospheric noise model.

Kenneth R. Olson



## Contents

	<u>Page</u>
Preface .....	ii
List of Figures .....	iv
List of Tables .....	v
Abstract .....	vi
I. Introduction .....	1
Objectives of Research .....	2
Background .....	2
Basic Research Strategy .....	4
II. Coherent M-ary Continuous-Phase Frequency Shift Keying Modulation .....	6
Modulation Description .....	6
Coherent Detection of M-ary CPFSK ...	7
III. Atmospheric Noise Model .....	10
Background .....	10
Rayleigh - Lognormal Mix Distribution Model .....	14
Rayleigh - Weibull Mix Distribution Model .....	25
IV. Performance Evaluation of the Receiver .	27
High-SNR Coherent Bound .....	27
Density of Random Variable Out of Correlators .....	28
Density Evaluation .....	30
Probability of Error Derivation .....	31
Numerical Solution of Probability of Error .....	32
Plotting Receiver Performance .....	34
V. Conclusions and Recommendations .....	40
Atmospheric Noise Models .....	40
M-ary CPFSK Receiver Performance ....	40
Bibliography .....	42
Appendix A .....	44
Vita .....	45

## List of Figures

<u>Figure</u>		<u>Page</u>
1	Optimum M-ary CPFSK Coherent Receiver for a Gaussian Channel .....	9
2	Example Plot of Amplitude Probability Distribution of the Envelope of Atmospheric Noise .....	11
3	Amplitude Probability Distributions of the Envelope of Atmospheric Noise for Various $V_d$ Ratios .....	13
4	Comparison of Distributions Obtained from Wilson's Data and from Equation (25) for $V_d = 4.0$ .....	23
5	Comparison of Distributions Obtained from Wilson's Data and from Equation (25) for $V_d = 5.0$ .....	24
6	Probability of Symbol Error for Quaternary Coherent CPFSK, $V_d = 4.0$ .....	36
7	Probability of Symbol Error for Quaternary Coherent CPFSK, $V_d = 5.0$ .....	37
8	Probability of Symbol Error Comparison with Schonhoff's Results .....	38

List of Tables

<u>Table</u>		<u>Page</u>
1	Parameters for Solution of Rayleigh - Lognormal Mix Distribution Model .....	25

### Abstract

Continuous-phase frequency shift keying (CPFSK) is potentially an attractive modulation scheme with performance better than Phase-shift keying (PSK) in Gaussian noise. The optimum coherent M-ary CPFSK receiver has been developed for operation in Gaussian noise. In this report the optimum receiver performance is evaluated assuming operation at very low frequencies.

Atmospheric noise is the most prevalent interference when operating at very low frequencies. An analytic amplitude probability distribution (APD) function is developed that closely approximates the Crichlow atmospheric noise APD model which is based on empirically measured data. The analytic expression for the APD was developed by combining a Rayleigh and a lognormal density and obtaining the corresponding distribution function. By correctly choosing values for two parameters in the distribution, it approximates the atmospheric noise APD for various  $V_d$  ratios (rms voltage/average voltage).

The performance of the optimum coherent M-ary CPFSK receiver was evaluated for  $M=4$  operating in atmospheric noise with specific  $V_d$  ratios (4 & 5). The evaluation consists of finding a probability of error bound for a sub-optimum receiver, which is valid for high signal-to-noise ratios (SNR). Results indicate



that the receiver performance in atmospheric noise becomes increasingly worse compared to performance in Gaussian noise as the SNR increases.

PERFORMANCE ANALYSIS OF CONTINUOUS-PHASE  
FREQUENCY SHIFT KEYING MODULATION  
IN ATMOSPHERIC NOISE

I. Introduction

There is a continuous search for signal modulation schemes that have improved performance. Performance is improved if a signal can be transmitted and received with the same error rate and bandwidth requirements but at a lower signal-to-noise ratio (SNR). Of course, the source and type of signal interference must be considered in evaluating performance.

Atmospheric radio noise is the major source of errors when operating at very low frequency (VLF). The physically massive, but electrically small, transmitting antennas required for operation at VLF are also a major concern. However, VLF communications systems do provide a reliable means of very long range surface-to-surface communications. Some of the attractive characteristics of radio transmission in the VLF band are (1) very low propagating signal attenuation rates, (2) minimal signal fading, and (3) very high signal phase stability (Ref 1:1). These characteristics make VLF communications systems a

good choice for providing command and control communications in times of war. Therefore, any improvements in performance of these systems are of major importance.

### Objectives of Research

One objective of this research is to develop an amplitude probability distribution (APD) function which characterizes atmospheric radio noise. Crichlow proposed an empirically based atmospheric noise distribution model based on attempts to identify known distributions which could be used to represent the probability distribution of the noise envelope voltage. The distribution function developed in this report should provide a model that corresponds with Crichlow's empirically based model (Refs 1:49-56; 3:5-8).

The second objective of this analysis is to evaluate the performance of continuous-phase frequency shift keying (CPFSK) modulation in the presence of atmospheric radio noise. Performance is evaluated by determining the symbol error probability as a function of signal power and noise power.

### Background

Although there have been many years of experience in VLF radio communications, few performance analyses of VLF communications systems operating in atmospheric

radio noise have been accomplished. This deficiency seems to exist because:

1. Emphasis was placed on higher frequencies for radio communications where atmospheric radio noise had little effect.
2. There is some practical difficulty in mathematically representing the atmospheric radio noise process, which is non-Gaussian and non-stationary over any extended period.
3. There are complications involved in using nonlinear receiver techniques to optimize signal demodulation. Since the detailed statistical characteristics of atmospheric noise are not known, optimum receivers were not designed for operation in an atmospheric noise environment. To overcome the effects of atmospheric noise, VLF system designers have used very high transmitter powers to compensate for inefficient receivers whose performance is drastically degraded by impulsive noise (Ref 1:2-5).

Recent studies indicate that CPFSK modulation can improve the efficiency of frequency shift keying (FSK) communications systems. Since FSK is generally used in VLF communications systems, it is important that any modulation scheme that improves efficiency be analyzed. CPFSK is a modulation scheme wherein the



phase is continuous between frequency shifts. By keeping the phase continuous, transient effects are reduced at the symbol transitions, and this provides spectral bandwidth advantages. Another important advantage of maintaining a continuous phase is that redundancy is imposed upon the waveform. Utilization of this redundancy allows a decision to be made upon the observation of several symbols rather than the more common approach of making a decision by looking at each symbol independently (Ref 4:644).

#### Basic Research Strategy

An attempt has been made to find an analytic expression for the atmospheric noise amplitude density that provides results comparable with the Crichlow graphical model. Crichlow proposed that the APD of atmospheric noise could be represented by two straight lines and a circular arc when plotted on probability paper upon which the Rayleigh complementary distribution function plots as a straight line (Refs 5:779; 2:50; 6:714). Wilson has developed a density function consisting of three different expressions that correspond to different regions of the curve (Ref 3:27-39). Although this density function consisting of one expression for the entire curve is more convenient to use in determining the performance of various receivers. Research has been based on the idea that the ends of the atmospheric noise APD curve approach

two specific distribution functions. Therefore the entire APD curve may possibly be represented by a distribution function that is based on a mixture of density functions corresponding to distribution functions approached at the ends of the curve.

Once an atmospheric noise amplitude density function has been determined, the performance of a CPFSK receiver can be determined. The CPFSK receiver is optimized for M-ary CPFSK when the interference is additive white Gaussian noise (Refs 7:1023-1036; 4:644-652).

This report is presented by chapters in the following sequence. Chapter II provides a description of the coherent CPFSK modulation scheme and of the optimum coherent M-ary CPFSK detector for an additive Gaussian channel. In Chapter III an atmospheric noise model is developed which provides results that closely approximate the Crichlow atmospheric noise model. The performance of the receiver described in Chapter II is evaluated in Chapter IV assuming that the interference is atmospheric noise. The atmospheric noise model developed in Chapter III is used in this evaluation. Chapter V provides conclusions of the study and recommends areas for further study.

## II. Coherent M-ary Continuous-Phase Frequency Shift Keying Modulation

The objective of this chapter is to present a description of M-ary CPFSK modulation and provide a brief description of the optimal coherent M-ary CPFSK detector presented by Schonhoff (Ref 4).

### Modulation Description

The M-ary CPFSK received signal can be modeled during the  $i^{\text{th}}$  signaling interval as:

$$r(t) = \left(\frac{2E}{T}\right)^{\frac{1}{2}} \cos\left(\omega_c t + \frac{d_i \pi h (t - (i-1)T)}{T} + h \sum_{j=1}^{i-1} d_j + \phi\right) + n(t),$$
$$(i-1)T \leq t < iT \quad (1)$$

where  $E$  - energy per signaling interval (symbol period)

$\omega_c$  - carrier radian frequency

$d_i$  - digital information signal ( $\pm 1, \pm 3, \dots, \pm(M-1)$ )  
in the  $i^{\text{th}}$  interval

$M$  - number of different  $d_i$ 's (always even)

$h$  - deviation ratio

$\phi$  - starting phase

$n(t)$  - additive noise

$T$  - signaling interval length or symbol period



The signal is constructed so that the separation between two adjacent frequencies in the M-ary set is  $h/T$  hertz. For coherent CPFSK the starting phase,  $\emptyset$ , can be assumed to be known and set to zero with no loss of generality. The shorthand notation developed by Osborne and Luntz (Ref 7:1024) for the received signal is used in this report.

$$r(t) = S(t, d, D_\alpha) + n(t) \quad (2)$$

where  $d$  is the first symbol and  $D_\alpha$  is the  $(n-1)$ -tuple  $D_\alpha = (d_2, d_3, \dots, d_n)$ . Equation (1) differs from Equation (2) in that Equation (2) represents the received signal over  $n$  symbol periods and Equation (1) represents the signal over one symbol period. Improved performance can be obtained with CPFSK modulation by observing the received signal for  $n$  symbol periods and making a decision on one of the symbols (Ref 4). In coherent detection of CPFSK signals, the decision is made on the first symbol.

#### Coherent Detection of M-ary CPFSK

The receiver design uses the fact that the carrier phase during the  $i^{\text{th}}$  bit time depends upon the data in the first bit time. Schonhoff (Ref 4:645-648) developed the optimum M-ary coherent detector for CPFSK assuming that the interference was additive white Gaussian noise. A block diagram of this receiver is given in Figure 1. In this figure the value of  $m$



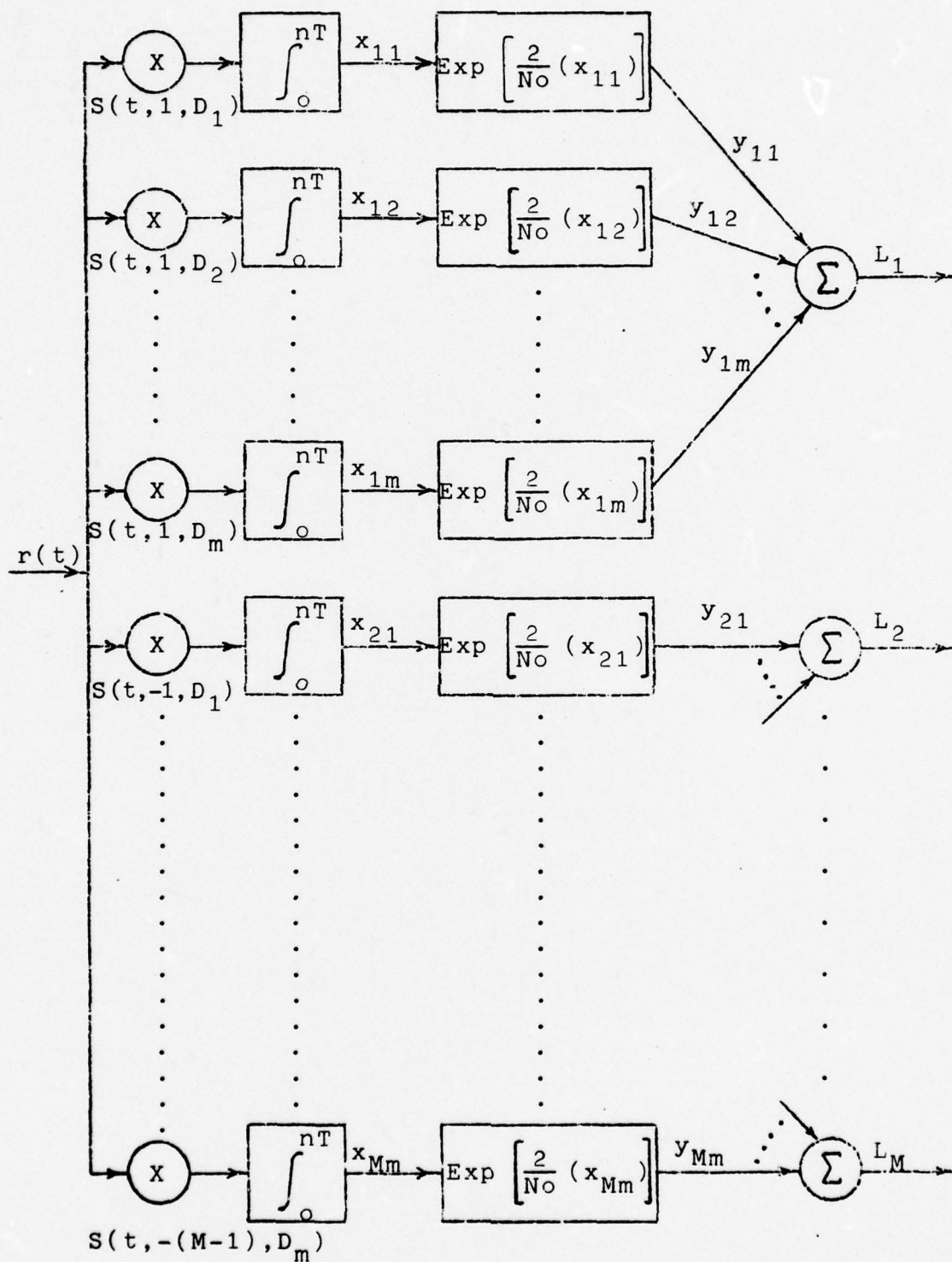


Figure 1. Optimum M-ary CPFSK Coherent Receiver for an Additive Gaussian Noise Channel

equals  $M^{n-1}$ , which is the number of possibilities for  $D_\alpha$ . The receiver correlates the received waveform with each of the  $m$  possible transmitted signals beginning with one of the  $d_i$  values. It then forms a  $k^{\text{th}}$  sum:

$$L_k = \sum_{j=1}^m \exp(2x_{kj}/N_0), \quad k=1 \dots M$$

$j=1 \dots m \quad (3)$

where  $x_{kj}$  is the correlation of the received waveform with the  $kj^{\text{th}}$  signal waveform. The decision of which data value was sent is determined by the largest sum,  $L_k$ .

The evaluation of this receiver's performance, when the additive noise,  $n(t)$ , is atmospheric noise, requires that at least the distribution and/or density of atmospheric noise be known.

### III. Atmospheric Noise Model

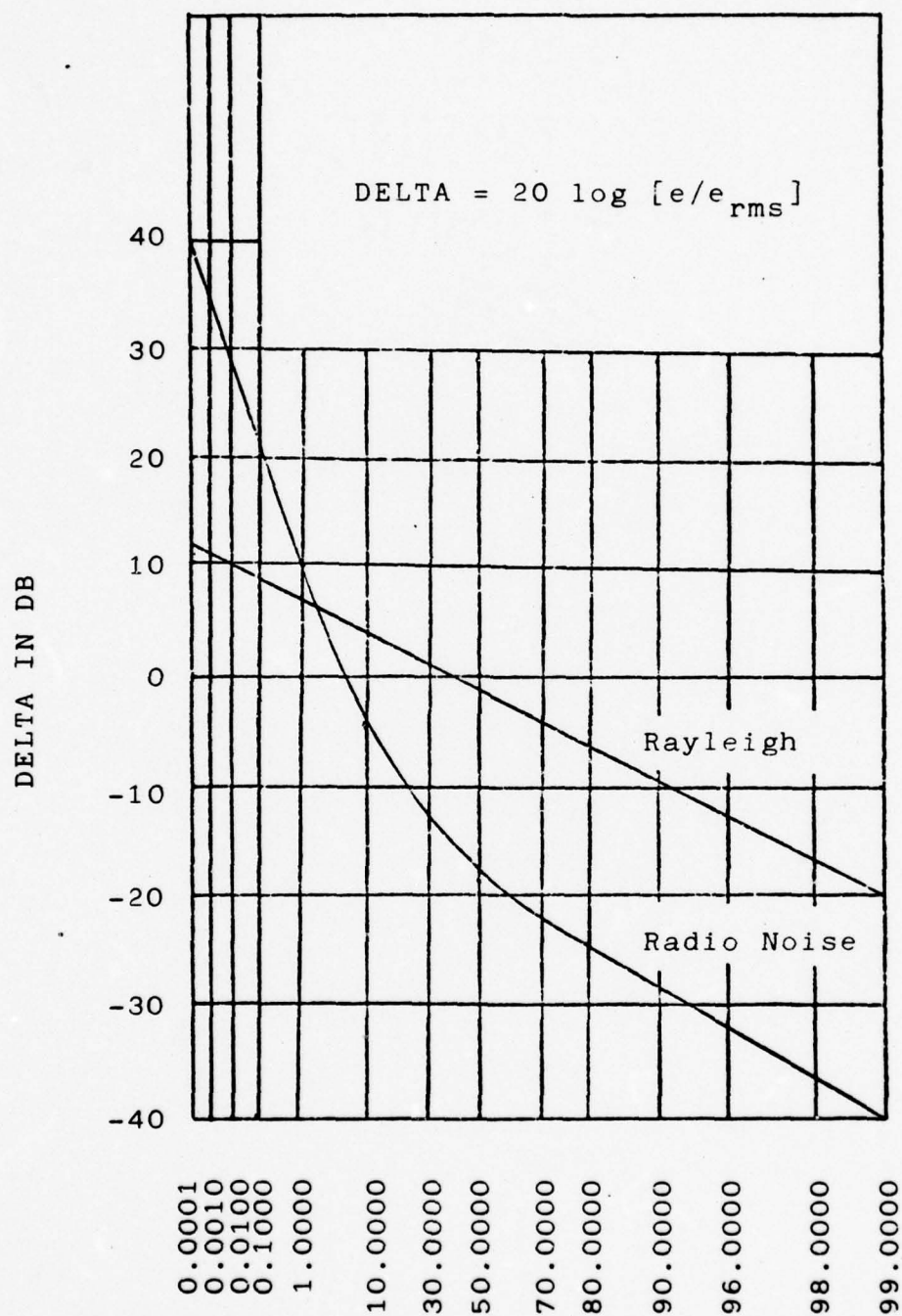
The objective of this chapter is to develop a mathematical atmospheric noise APD model that agrees with the Crichlow model. The model will be used to determine the performance of a CPFSK receiver, optimized for an additive Gaussian noise channel, while operating in an atmospheric noise environment.

#### Background

Crichlow's atmospheric noise APD model describes the statistical properties of the amplitude distribution of atmospheric radio noise. The data used to develop this model consisted of measurements of exceedance probability

$$P \left[ \frac{e}{e_{rms}} > R \right] \quad (4)$$

made during the International Geophysical Year. Crichlow noted that the APD could be approximated by two straight lines and a circular arc when plotted on paper where a Rayleigh distribution function plots as a straight line with slope equal to minus one-half (Refs 5:778-780; 2:49-50). An example plot is given in Figure 2. The lower portion of the curve represents low voltages with high exceedance probabilities; these



PERCENTAGE OF TIME FOR WHICH DELTA IS EXCEEDED

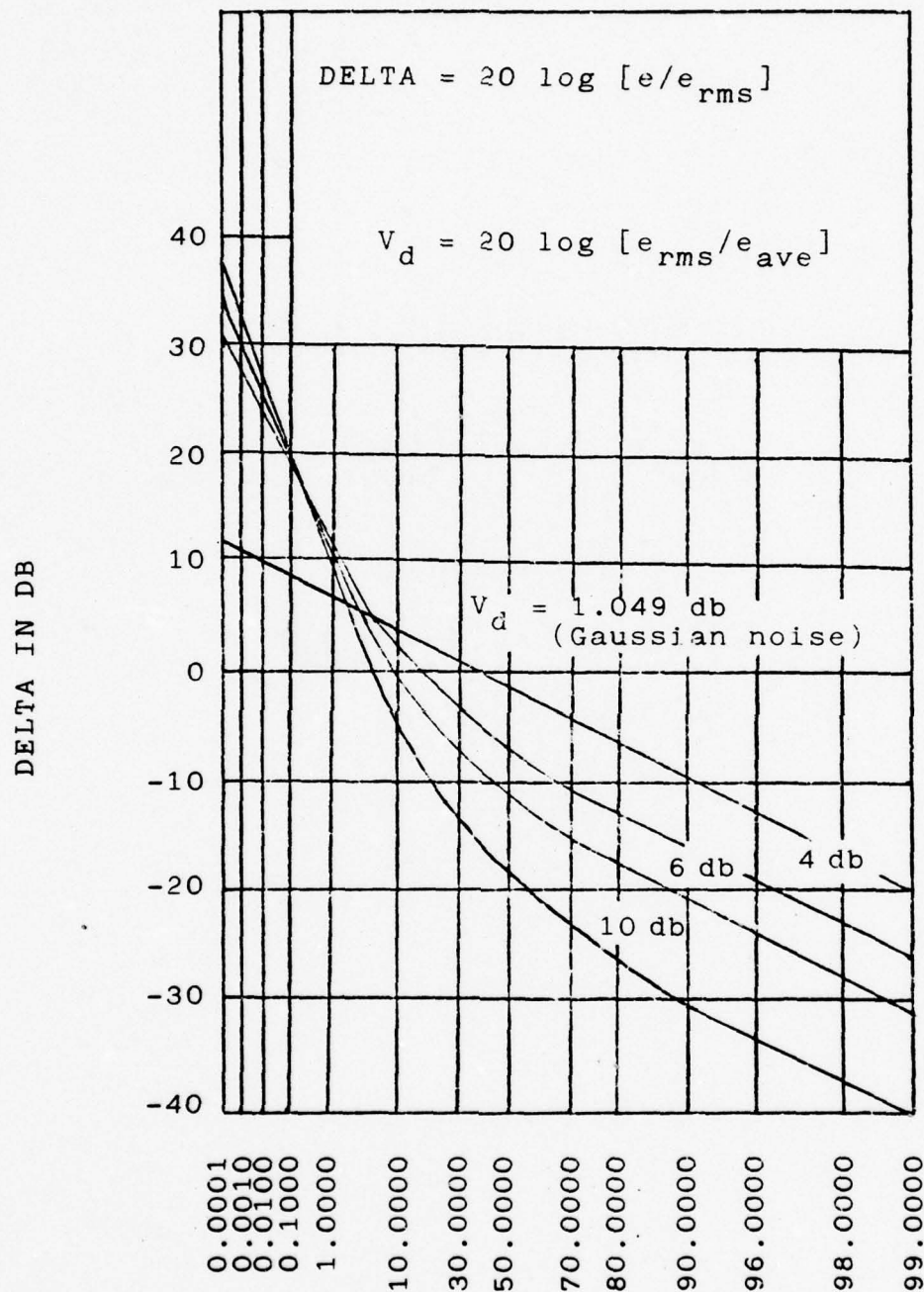
Figure 2. Example Plot of Amplitude Probability Distribution of the Envelope of Atmospheric Noise



approach a Rayleigh distribution. The upper portion of the curve represents very high voltages with low exceedance probabilities; these approach a lognormal or Weibull distribution.

The APD curve varies depending upon the closeness of atmospheric noise generators (lightning discharges, etc). As the lightning discharges occur closer to the measuring device, the atmospheric noise is more impulsive. This noise impulsiveness is described by an impulsiveness form factor,  $V_d$ , defined to be the ratio of the root mean square (rms) noise envelope voltage to the average (ave) noise envelope voltage (Ref 3:37-38). Figure 3 shows typical APD curves plotted on Rayleigh paper for various  $V_d$  ratios. These curves show that as the  $V_d$  ratio increases, the APD of atmospheric noise changes in a predictable way.

Wilson developed the expressions for the three regions suggested by Crichlow and determined the boundary points between the regions for various  $V_d$  ratios (Ref 3:27-37). He represented the low voltage, high probability, straight line portion of the curve by a Rayleigh expression. The high exceedance, low probability, straight line portion of the curve was represented by a Weibull expression. The center portion of the curve was represented by a circular arc expression. From these three expressions, a density function was developed to use in evaluating receiver performance.



PERCENTAGE OF TIME FOR WHICH DELTA IS EXCEEDED

Figure 3. Amplitude Probability Distributions of the Envelope of Atmospheric Noise for Various  $V_d$  Ratios

Using Wilson's noise density function to evaluate performance of various receivers is not convenient. It is advantageous to find a single expression that represents an entire APD curve. The APD curve for each  $V_d$  ratio could be obtained by changing the parameters of this function.

#### Rayleigh - Lognormal Mix Distribution Model

Beckmann noted, as Crichlow and Wilson had, that the low exceedance, high probability, straight line portions of Crichlow's APD curves were Rayleigh distributed. However, he found that the high exceedance, low probability portions of the APD curves could be approximated by a lognormal distribution (Ref 8:723-724). Therefore in this report it was assumed that instantaneous density functions, associated with both the Rayleigh and lognormal distribution functions, could be properly combined into one density function for the entire curve. In the following derivation of this mixed density function, it is assumed that the phase of the instantaneous atmospheric noise voltage is uniformly distributed and independent of the amplitude. This assumption is made for expediency since there is no known relationship between noise amplitude and phase.

If the atmospheric noise APD is Rayleigh, then the atmospheric noise amplitude density is (Ref 9:49-50)

$$p_z(z) = \frac{2z}{A} \exp [-z^2/A], \quad z \geq 0 \quad (5)$$

where  $z$  is the noise amplitude voltage. If the instantaneous atmospheric noise phase is considered to be uniformly distributed, the density function of the phase is

$$p_\phi(\phi) = \frac{1}{2\pi}, \quad 0 \leq \phi \leq 2\pi \text{ and zero elsewhere} \quad (6)$$

By using the assumption that the amplitude,  $z$ , and phase,  $\phi$ , of atmospheric noise to be independent, the joint density is obtained by simply multiplying the densities, (Equations (5) and (6)) together.

$$p_{z,\phi}(z,\phi) = \frac{z}{A\pi} \exp[-z^2/A], \quad z \geq 0 \\ 0 \leq \phi \leq 2\pi \quad (7)$$

This joint density function can be transformed into a joint density function with in-phase and quadrature components of the noise. The transformed density is sometimes referred to as an instantaneous density. The in-phase and quadrature components of this density function will be added to the in-phase and quadrature components of an instantaneous density function obtained from the lognormal distribution. The transformation is accomplished by letting  $x = z \cos \phi$  and  $y = z \sin \phi$  (Ref 9:10-12). Therefore the instantaneous



density is

$$p_{\underline{x}, \underline{y}}(x, y) = |J| p_{\underline{z}, \underline{\theta}}((x^2 + y^2)^{1/2}, \tan^{-1}(y/x)) \quad (8)$$

where

$$|J| = 1/(x^2 + y^2)^{1/2} \quad (9)$$

the Jacobian of the transformation, thus

$$p_{\underline{x}, \underline{y}}(x, y) = \frac{1}{A\pi} \exp \left[ -\frac{x^2 + y^2}{A} \right] \quad (10)$$

If the atmospheric noise APD is lognormal, then the atmospheric noise amplitude density is (Ref 10:50)

$$p_{\underline{z}}(z) = \frac{1}{zs(2\pi)^{1/2}} \exp \left[ -\frac{(\ln(z)-a)^2}{2s^2} \right], \quad z > 0, \quad s > 0 \quad (11)$$

Again it is assumed that the instantaneous atmospheric noise phase is uniformly distributed and independent of the amplitude. The joint density is obtained by multiplying densities, Equation (6) and Equation (11), together and obtaining

$$p_{\underline{z}, \underline{\theta}}(z, \theta) = \frac{1}{2sz\pi(2\pi)^{1/2}} \exp \left[ -\frac{(\ln(z)-a)^2}{2s^2} \right], \quad z > 0, \quad 0 \leq \theta \leq 2\pi \quad (12)$$

This joint density must also be transformed into an instantaneous density function as was done in the Rayleigh case. This results in

$$p_{\underline{x}, \underline{y}}(x, y) = \frac{1}{s(x^2 + y^2) 2\pi(2\pi)^{1/2}} \exp\left[-\frac{(\ln((x^2 + y^2)^{1/2}) - a)^2}{2s^2}\right] \quad (13)$$

Assume that  $\underline{x}_1$  and  $\underline{y}_1$  are the random variables in Equation (10) and  $\underline{x}_2$  and  $\underline{y}_2$  are the random variables in Equation (13). An instantaneous mixed density function with random variables  $\underline{u}$  and  $\underline{v}$  can be obtained by letting  $\underline{u} = \underline{x}_1 + \underline{x}_2$  and  $\underline{v} = \underline{y}_1 + \underline{y}_2$ . Since densities given by Equations (10) and (13) are considered independent, the instantaneous mixed density is obtained by convolving the densities (Ref 11:188-189).

$$p_{\underline{u}, \underline{v}}(u, v) = \iint_{-\infty}^{\infty} p_{\underline{x}, \underline{y}}(x, y) p_{\underline{x}, \underline{y}}(u-x, v-y) dx dy \quad (14)$$

Substituting Equation (13) for the first density and Equation (10) for the second density

$$p_{\underline{u}, \underline{v}}(u, v) = \iint_{-\infty}^{\infty} \frac{1}{2\pi(2\pi)^{1/2} s(x^2 + y^2)} \exp\left[-\frac{(\ln(x^2 + y^2)^{1/2} - a)^2}{2s^2}\right] \cdot \frac{1}{A\pi} \exp\left[-\frac{(u-x)^2 + (v-y)^2}{A}\right] dx dy \quad (15)$$

This resulting density function, Equation (15), must now be transformed into a joint density of magnitude and phase random variables. This is done by

letting  $\underline{u} = \underline{z} \cos \underline{\theta}$ ,  $\underline{v} = \underline{z} \sin \underline{\theta}$  and applying the general transformation equation (Ref 12:96).

$$p_{\underline{z}, \underline{\theta}}(z, \theta) = |J| p_{\underline{u}, \underline{v}}(\underline{z} \cos \underline{\theta}, \underline{z} \sin \underline{\theta}) \quad (16)$$

where  $|J| = z$ , the Jacobian of the transformation.

Thus

$$p_{\underline{z}, \underline{\theta}}(z, \theta) = \frac{z}{2\pi^2 (2\pi)^{1/2} s_A} \iint_{-\infty}^{\infty} \frac{1}{x^2 + y^2} \cdot \exp \left[ - \frac{(\ln(x^2 + y^2)^{1/2} - a)^2}{2s^2} \right] \exp \left[ - \frac{((z \cos \theta - x)^2 + (z \sin \theta - y)^2)}{A} \right] dx dy, \quad z \geq 0$$

$$0 \leq \theta \leq 2\pi \quad (17)$$

The last term of Equation (17) can be easily expanded and simplified to

$$\exp \left[ - \frac{z^2}{A} \right] \exp \left[ \frac{x^2 + y^2}{A} \right] \exp \left[ \frac{2z}{A} (x \cos \theta + y \sin \theta) \right] \quad (18)$$

By substituting Equation (18) for the last term of Equation (17) the joint density becomes

$$p_{\underline{z}, \underline{\theta}}(z, \theta) = \frac{z}{2\pi^2 (2\pi)^{1/2} s_A} \exp \left[ - \frac{z^2}{A} \right] \iint_{-\infty}^{\infty} \frac{1}{x^2 + y^2} \cdot \exp \left[ - \frac{(\ln(x^2 + y^2)^{1/2} - a)^2}{2s^2} \right] \cdot \exp \left[ - \frac{x^2 + y^2}{A} \right] \exp \left[ \frac{2z}{A} (x \cos \theta + y \sin \theta) \right] dx dy, \quad z \geq 0$$

$$0 \leq \theta \leq 2\pi \quad (19)$$

To obtain the density of the amplitude of atmospheric noise, the random variable  $\underline{\theta}$ , must be integrated out of density Equation (19).

$$p_{\underline{z}}(z) = \frac{z}{2\pi^2 (2\pi)^{1/2} sA} \exp\left[-\frac{z^2}{A}\right] \iint_{-\infty}^{\infty} \frac{1}{x^2 + y^2} \cdot \exp\left[-\frac{(\ln(x^2 + y^2)^{1/2} - a)^2}{2s^2}\right] \exp\left[-\frac{x^2 + y^2}{A}\right] \cdot \int_0^{2\pi} \exp\left[\frac{2z}{A} (x \cos \theta + y \sin \theta)\right] d\theta dx dy, \quad z \geq 0 \quad (20)$$

The last term in Equation (19) can be simplified to the following expression by a change of variable and using the definition of a modified Bessel function.

$$2\pi I_0\left[\frac{2z(x^2 + y^2)^{1/2}}{A}\right] \quad (21)$$

Further simplification can be made to Equation (20) by changing to polar coordinates. The atmospheric noise amplitude density is now

$$p_{\underline{z}}(z) = \frac{z}{\pi (2\pi)^{1/2} sA} \exp\left[-\frac{z^2}{A}\right] \int_0^{\infty} \int_0^{2\pi} \frac{1}{r} \cdot \exp\left[-\frac{(\ln(r) - a)^2}{2s^2}\right] \exp\left[-\frac{r^2}{A}\right] I_0\left[\frac{2zr}{A}\right] d\theta dr, \quad \begin{matrix} z \geq 0 \\ r \geq 0 \end{matrix} \quad (22)$$



Since  $\theta$  does not appear in Equation (22), it is easily integrated out to give

$$p_z(z) = \frac{2z}{(2)^{1/2} s A} \exp \left[ -\frac{z^2}{A} \right] \int_0^\infty \frac{1}{r} \exp \left[ -\frac{(\ln(r)-a)^2}{2s^2} \right] \cdot \exp \left[ -\frac{r^2}{A} \right] I_0 \left[ \frac{2zr}{A} \right] dr \quad (23)$$

The root mean square value of the noise amplitude,  $z$ , that is lognormal distributed, is (Ref 3:115-116).

$$z_{rms} = z^a z^{s^2} \quad (24)$$

Therefore, if the root mean square value of the noise amplitude is normalized to equal 1,  $a = -s^2$ . By making this substitution, the number of parameters in Equation (23) can be reduced from three to two. The corresponding probability of exceedance is

$$P \left[ \frac{z}{z_{rms}} > R \right] = \frac{2}{As(2\pi)^{1/2}} \int_R^\infty \int_0^\infty \frac{z}{r} \exp \left[ -\frac{z^2 + r^2}{A} - \frac{(\ln(r) + s^2)^2}{2s^2} \right] \cdot I_0 \left[ \frac{2zr}{A} \right] dr dz \quad (25)$$

Analytical attempts at finding a closed form solution to Equation (23) and (25) failed. If the substitutions  $z=E$ ,  $z_{rms}=E_{rms}$ ,  $r=E_0$ ,  $s^2=\sigma^2$ , and  $A=N_c$  are made in Equation (25), the resulting equation is identical to

Beckmann's Equation (5.19) in Reference 8. This equation is the final solution Beckmann derived to represent the APD of atmospheric noise.

To determine the particular values of parameters A and s for specific  $V_d$  ratios, the average and root mean square values of the noise amplitude are solved using

$$z_{ave} = \int_0^{\infty} z p_z(z) dz \quad (26)$$

$$z_{rms} = \text{square root of} \left[ \int_0^{\infty} z^2 p_z(z) dz \right] \quad (27)$$

and this allowed calculation of the  $V_d$  ratio

$$V_d = 20 \log \left[ \frac{z_{rms}}{z_{ave}} \right] \quad (28)$$

Equations (25), (26), (27), and (28) were solved numerically, using Air Force Institute of Technology single and double integration programs. These two computer programs use Simpson's rule and are identified as SIMPS and SIMPD respectively. The modified Bessel function of the first kind of order zero ( $I_0$ ) was evaluated using the function program in Appendix A. This program is developed from numerical equations for

evaluating  $I(x)$  (Ref 13:377-378). Numerical solutions are accurate to at least six decimal places.

With variables  $r$  and  $z$  integrated from 0.001 to 26.0, the probability of exceedance is plotted for various combinations of  $A$  and  $s$ . The correct combination of values for  $A$  and  $s$  are obtained when the following two requirements are met.

- 1)  $z_{rms} \approx 1$
- 2) For specific  $V_d$  ratios the APD curves obtained, using Equation (25), must match the APD curves from Crichlow's model.

Although this may seem relatively simple, it is highly improbable that the exact combination of values will be found by this numerical method. Since Equations (25), (26), and (27) were not numerically integrated out to infinity, the most that can be hoped for is to obtain values of  $A$  and  $s$  which will allow close approximation to the Crichlow APD curves. Calculations for the higher  $V_d$  ratios requires a large amount of computer processing time, thus approximate values for  $A$  and  $s$  are obtained only for  $V_d$  ratios of four and five. These values are listed in Table I. Since the APD curves obtained by Wilson appear to be identical to the Crichlow curves, Wilson's curves are used for comparison purposes. A computer plot comparison of the APD curves obtained from Wilson's data (Ref 3:45) and from Equation (25) are given in Figures 4 and 5.

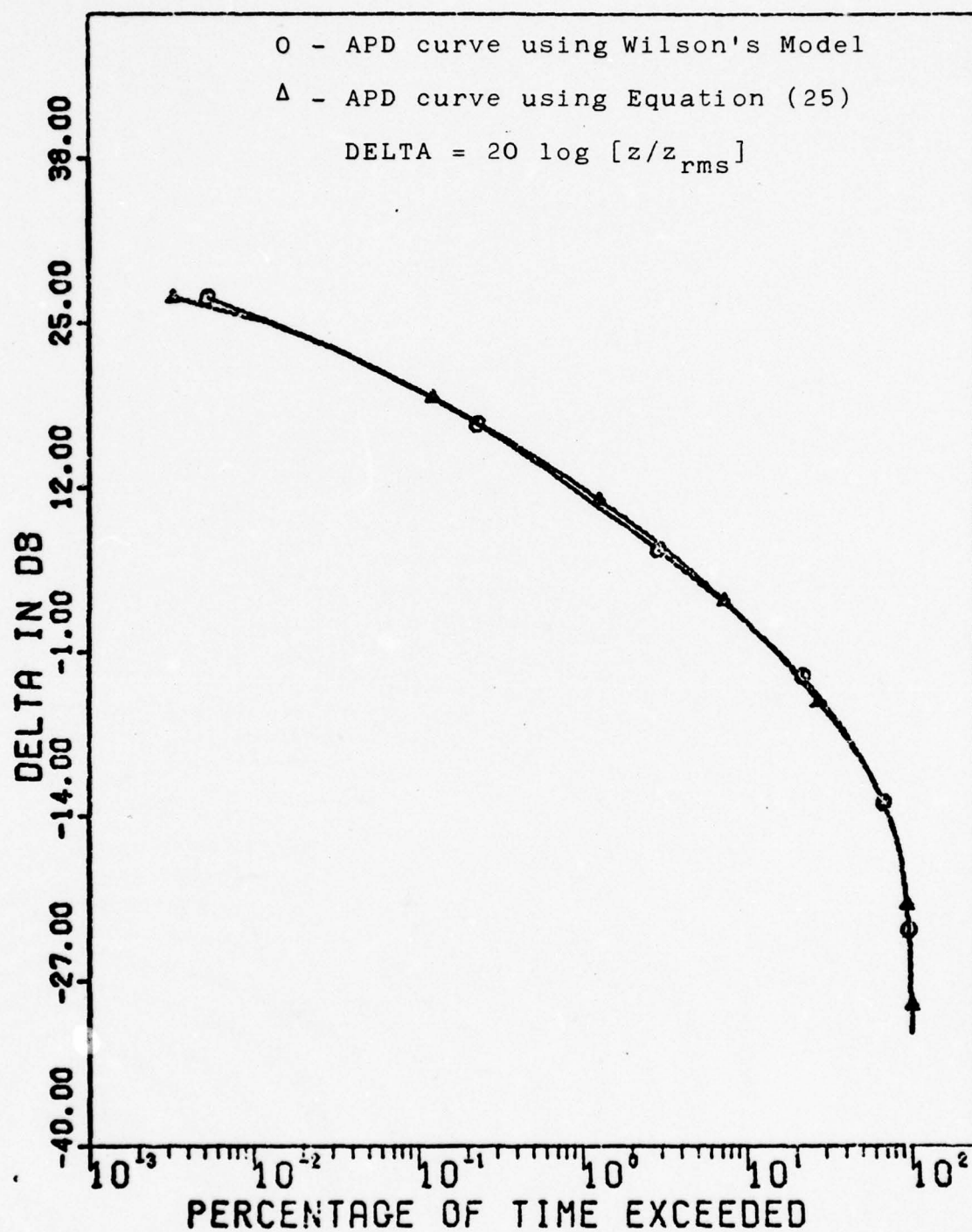


Figure 4. Comparison of Distributions Obtained From Wilson's Model and from Equation 25 for  $V_d = 4.0$



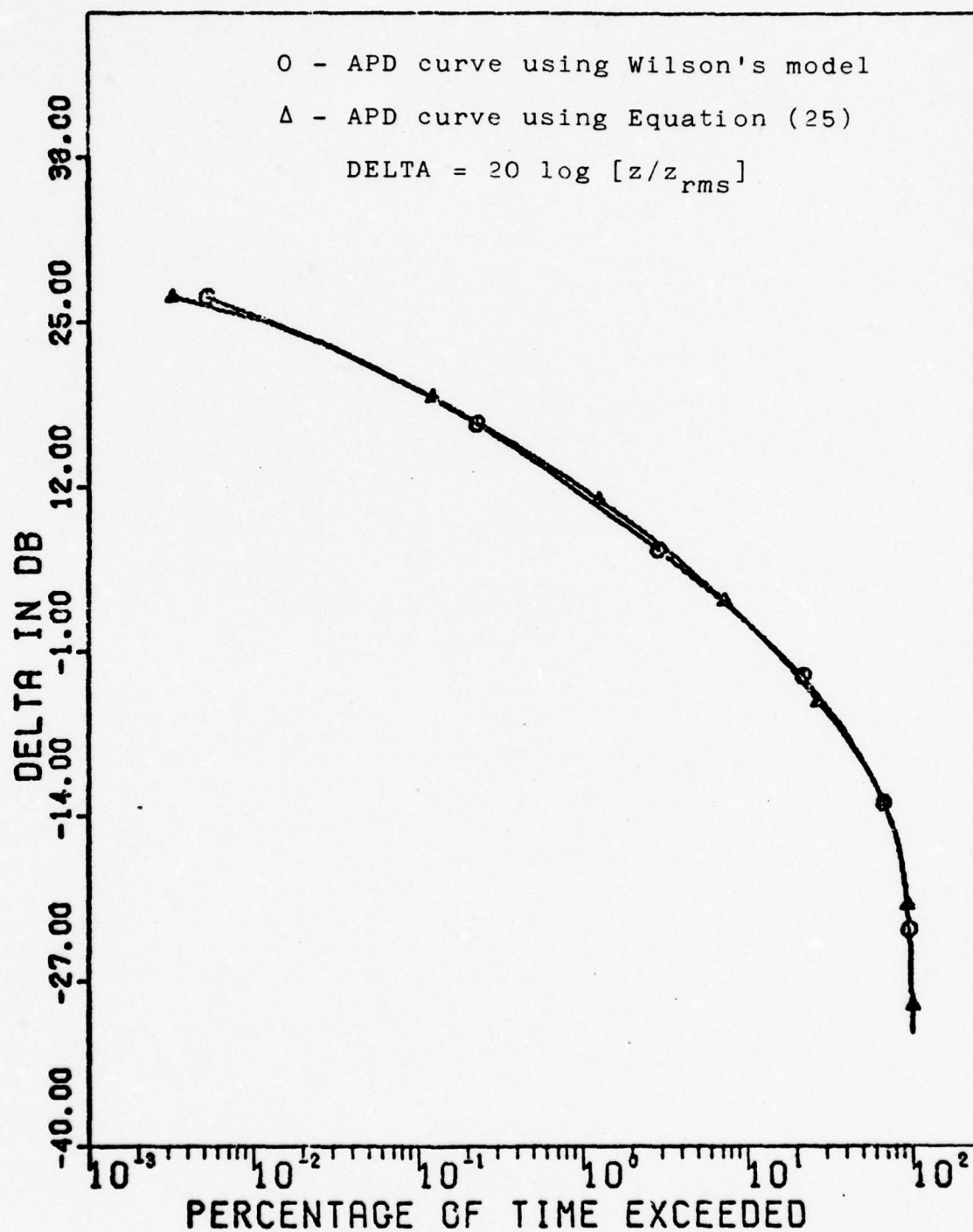


Figure 5. Comparison of Distributions Obtained from  
 Wilson's Model and from Equation (25)  
 for  $V_d = 5.0$

Table I

Parameters for Solution of Rayleigh-  
Lognormal Mix Distribution Model

$V_d$	A	s
4.0	0.0973	1.09
5.0	0.04	1.19

Rayleigh - Weibull Mix Distribution Model

As suggested by Wilson, the low exceedance probability portion of the APD curves can be approximated by a Weibull distribution. Again assuming that the phase of the instantaneous noise voltage is uniformly distributed and independent of amplitude, the instantaneous density of the Weibull distribution is

$$p_{x,y}(x,y) = \frac{a}{4\pi} (x^2 + y^2)^{(b/2)-1} \exp \left[ -a(x^2 + y^2)^{b/2} \right] \quad (29)$$

where a and b are parameters of the function (Ref 12: 216). Using this density and the instantaneous Rayleigh density, Equation (7), the process of convolution and transformations were accomplished as before. The resulting amplitude density function obtained was

$$p_z(z) = \frac{za}{A} \int_0^{\infty} r(r^2)^{(b/2)-1} \exp\left[-a(r^2)^{b/2}\right] \exp\left[-\frac{r^2}{A}\right] I_0\left[\frac{2zr}{A}\right] dr, \quad z \geq 0 \quad (30)$$

The resulting equation for the probability of exceedance is thus given by

$$P\left[\frac{z}{z_{rms}} > R\right] = \frac{a}{A} \int_R^{\infty} \int_0^{\infty} zr(r^2)^{(b/2)-1} \exp\left[-a(r^2)^{b/2}\right] \exp\left[-\frac{r^2}{A}\right] I_0\left[\frac{2zr}{A}\right] dr dz, \quad z \geq 0 \quad (31)$$

Again no closed form solutions could be found for Equations (30) or (31). Attempts were made to obtain the proper combination of values for  $a$ ,  $A$ , and  $b$  to obtain approximations for the various APD curves. However, due to the time constraints of completing this report, the many possible combinations of the parameter values, and the large amount of processing time required, the search for the proper combinations of parameter values was soon dropped.

#### IV. Performance Evaluation of the Receiver

The objective of this chapter is to evaluate the performance of the receiver described in Chapter II when the signal interference is caused by atmospheric noise. The lognormal-Rayleigh atmospheric noise mix model developed in Chapter III is used in this evaluation. It is not possible to analyze the performance of the receiver exactly. However, bounds on performance can be determined for high and low SNR. Due to time constraints, only the high SNR bound is developed in this report. Developing a low SNR bound is more complex and requires the development of a density function for the summer outputs,  $\underline{L}$ 's, as depicted in Figure 1.

##### High-SNR Coherent Bound

Reference Figure 1 the M likelihood parameters can be written as (Ref 4:646)

$$\underline{L}_k = \sum_{j=1}^m \exp \left[ \frac{2}{N_o} \underline{x}_{kj} \right], \quad k=1, \dots, M \quad (32)$$

For large SNR,

$$\sum_{j=1}^m \exp \left[ \frac{2}{N_o} \underline{x}_{kj} \right] \approx \exp \left[ \frac{2}{N_o} \underline{x}_o \right] \quad (33)$$



where  $\underline{x}_0$  is the largest of the  $\underline{x}_{kj}$ . Since the exponential function is a monotonic function,  $\underline{x}_0$  is an equivalent parameter to investigate. If the receiver simply picks the largest  $\underline{x}_{kj}$  and makes a decision on  $d$ , it is a suboptimum receiver.

#### Density of Random Variable Out of Correlators

To evaluate the performance of the receiver, the density of  $\underline{x}_{kj}$  must be determined.

$$\underline{x}_{kj} = \int_0^{nT} \underline{r}(t) S(t, k, D_j) dt \quad (34)$$

Assuming that the transmitted signal is  $S(t, d, D)$ , where  $D = \{d_2, d_3, \dots, d_n\}$ ,  $\underline{x}_{kj}$  is given by

$$\underline{x}_{kj} = \int_0^{nT} S(t, d, D) S(t, k, D_j) dt + \int_0^{nT} S(t, k, D_j) \underline{n}(t) dt \quad (35)$$

If the correlation is defined to be

$$\rho_{kjdD} = \frac{1}{nE} \int_0^{nT} S(t, d, D) S(t, k, D_j) dt \quad (36)$$

Then Equation (35) becomes

$$\underline{x}_{kj} = \rho_{kj} d D^{En} + \int_0^{nT} S(t, k, D_j) \underline{n}(t) dt \quad (37)$$

The integral in Equation (37) is now defined as a random variable,  $\underline{c}_{kj}$

$$\underline{c}_{kj} = \int_0^{nT} S(t, k, D_j) \underline{n}(t) dt \quad (38)$$

The density of  $\underline{c}_{kj}$  is equal to the in-phase or quadrature component of the instantaneous atmospheric noise density, since Equation (38) can be considered a narrowband process. The instantaneous atmospheric noise density is given by Equation (15). By letting  $r^2 = x^2 + y^2$ ,  $u=x$ , and  $v=y$  Equation (15) is simplified to

$$p_{\underline{x}, \underline{y}}(x, y) = \frac{2}{A \pi s (2\pi)^{1/2}} \int_0^{\infty} \frac{1}{r} \exp \left[ -\frac{(\ln(r) + s^2)^2}{2s^2} - \frac{(x^2 + y^2 + r^2)}{A} \right] I_0 \left[ \frac{2r(x^2 + y^2)^{1/2}}{A} \right] dr \quad (39)$$

The density of  $\underline{c}_{kj}$  is then just the marginal density derived from Equation (39).

$$p_{\underline{c}_{kj}}(x) = \frac{2}{A\pi s(2\pi)^{1/2}} \int_{-\infty}^{\infty} \int_0^{\infty} \frac{1}{r} \exp \left[ -\frac{(\ln(r) + s^2)^2}{2s^2} - \frac{(x^2 + y^2 + r^2)}{A} \right] I_0 \left[ \frac{2r(x^2 + y^2)^{1/2}}{A} \right] dr dy \quad (40)$$

This density has zero mean and is symmetric about the origin. The density of  $\underline{x}_{kj}$  is given by (Ref 12:181)

$$p_{\underline{x}_{kj}}(x) = p_{\underline{c}_{kj}}(x - \rho_{kj dD} nE) \quad (41)$$

In words,  $\underline{x}_{kj}$  has the same form as the density of  $\underline{c}_{kj}$  except it is shifted by  $\rho_{kj dD} nE$ .

Density Evaluation. Equation (41) shows that the densities  $p_{\underline{x}_{dD}}$  and  $p_{\underline{x}_{kj}}$  are identical in form, but they have different means which are determined by the correlation,  $\rho_{kj dD}$ . In the numerical evaluation of the density function, Equation (40),  $r$  was integrated out to 15 and  $y$  was integrated from -10 to +10 using the Air Force Institute of Technology double integration program, SIMPD.

The density function, Equation (40), was evaluated at 197 equally spaced points between -10 and +10. The limits chosen for  $r$ ,  $y$ , and  $x$  are picked to keep integration time to a minimum and still have at least two

significant figures in the results. Two significant figures are considered sufficient, since greater accuracy cannot be obtained from Crichlow's curves.

#### Probability of Error Derivation

Assuming that  $d=v$  and  $D=\{d_2, d_3, \dots, d_n\}$  for the transmitted data sequence, the probability of error is given by the following equation.

$$P[\epsilon | S(t, v, D)] = P[\text{any } \underline{x}_{kj} > \underline{x}_{vD}] \quad (42)$$

Applying the union bound (Ref 14:263-264).

$$P[\epsilon | S(t, v, D)] < \sum_{\substack{k=1 \\ k \neq v}}^M \sum_{j=1}^m P[\underline{x}_{kj} > \underline{x}_{vD}] \quad (43)$$

or

$$P[\epsilon | S(t, v, D)] < \sum_{\substack{k=1 \\ k \neq v}}^M \sum_{j=1}^m \int_{-\infty}^{\infty} \int_x^{\infty} p_{\underline{x}_{kj}, \underline{x}_{vD}}(x, y) dx dy \quad (44)$$

However, the joint densities of different combinations of the correlator outputs are not known. Therefore, a worst case situation will be assumed, i.e. the  $\underline{x}_{kj}$  are assumed to be independent. This worst case condition will give an upper bound on the probability of error since the correlation between the  $\underline{x}_{kj}$ 's are being



ignored. The probability of error is then given by

$$P[\epsilon | S(t, v, D)] = \sum_{\substack{k=1 \\ k \neq v}}^M \sum_{j=1}^m \int_{-\infty}^{\infty} p_{\underline{x}_{vD}}(x) \int_x^{\infty} p_{\underline{x}_{kj}}(y) dy dx \quad (45)$$

Then by averaging the conditional probability of error over all possible input signals, an expression for the probability of error is obtained that is independent of the input signal.

$$P[\epsilon] = \sum_{\substack{k=1 \\ k \neq v}}^M \sum_{j=1}^m \sum_{v=1}^M \sum_{D=1}^m \int_{-\infty}^{\infty} p_{\underline{x}_{vD}}(x) \int_x^{\infty} p_{\underline{x}_{kj}}(y) dy dx \quad (46)$$

#### Numerical Solution of Probability of Error

The bound on probability of error for M-ary CPFSK is solved numerically for M=4, n=3, and h=0.8. The value used for h was found by Schonhoff to be the optimum value for quaternary modulation and n=3 in an additive Gaussian noise channel.

Before the bound on the probability of error can be determined, Equation (36) for the correlation must be solved. A symbol-by-symbol correlation was performed using the equations developed by Schonhoff (Ref 4:647). However it was noted that Schonhoff's equations for b and d are incorrect. The  $\pi h$  factor should be divided out of each equation, making them

$$b = N + \sum_{\ell=2}^{n-1} d_{\ell J} \quad (47)$$

$$d = v + \sum_{\ell=2}^{n-1} d_{\ell J} \quad (48)$$

With the correlations determined, the means of densities  $p_{\underline{x}_{vD}}(x)$  and  $p_{\underline{x}_{kj}}(x)$  are

$$M_{\underline{x}_{vD}} = \rho_{kj d D} n E, \quad \begin{matrix} k = d \\ j = D \end{matrix} \quad (49)$$

$$M_{\underline{x}_{kj}} = \rho_{kj d D} n E, \quad k \neq d \quad (50)$$

To obtain a numerical solution to the inequality Equation (46), the integrals are changed to summations with limits which will cover the non-zero area.

$$P[\epsilon] = \sum_{\substack{k=1 \\ k \neq v}}^M \sum_{j=1}^m \sum_{v=1}^M \sum_{D=1}^m$$

$$\sum_{x=M_{\underline{x}_{vD}}-10}^{M_{\underline{x}_{kj}}+10} p_{\underline{x}_{vD}}(x) \sum_{y=x}^{M_{\underline{x}_{kj}}+10} p_{\underline{x}_{kj}}(y) \Delta y \Delta x \quad (51)$$

Since the numerical solution of inequality Equation (51) requires a large amount of computer time, the probability of error bound is calculated by averaging over 8 randomly picked input signals instead of the 64 total possible signals. Probability of error solutions obtained by averaging over 8 randomly picked input signals were compared with solutions obtained by averaging over different groups of 8 randomly picked input signals. This comparison revealed that the probability of error differed only in the third significant digit. Therefore it is assumed that this approximation does not effect the results appreciably. The inequality Equation (51) is reduced to

$$P[\epsilon] = \sum_{\substack{k=1 \\ k \neq v}}^M \sum_{j=1}^m \sum_{\substack{\text{(over 8 arbitrary)} \\ \text{input signals}}} \sum_{x=M}^{\sum_{k,j} x_{kj} + 10} p_{x_{vD}}(x) \cdot$$

$$\sum_{y=x}^{\sum_{k,j} x_{kj} + 10} p_{x_{kj}}(y) \Delta y \Delta x. \quad (52)$$

### Plotting Receiver Performance

Receiver performance is displayed by plotting probability of error bound versus SNR. The SNR is expressed as the energy per symbol interval divided

by the variance of the atmospheric noise density, Equation (40). It is assumed that the energy in each symbol interval was normalized to one and therefore there is equal energy in each symbol interval.

Performance plots for  $V_d = 4.0$  and  $V_d = 5.0$  are shown in Figures 6 and 7, respectively. The performance is also plotted for Gaussian noise with variance equal to the variance of the respective noise densities used for comparison.

Figures 6 and 7 clearly indicate that the upper bounds on probability of error for atmospheric noise and Gaussian noise come closer together as the SNR decreases. At  $SNR = 0$  the upper bound for each is almost identical. The implication of the performance curves is that if the receiver is used in an additive atmospheric noise environment, then a higher SNR will have to be maintained to obtain the same probability of error as predicted for its use in a Gaussian channel.

It is noted that the Gaussian noise curves for  $M=4$ ,  $n=3$ , and  $h=0.8$  are identical for different variances. This result is expected since the probability of error is plotted versus SNR. However, the Gaussian noise curves obtained in Figures 6 and 7 are not identical to Schonhoff's curve (Ref 4:648). A curve comparison is given in Figure 8, which shows that for a  $SNR \leq 2.0$  Schonhoff obtains a lower probability



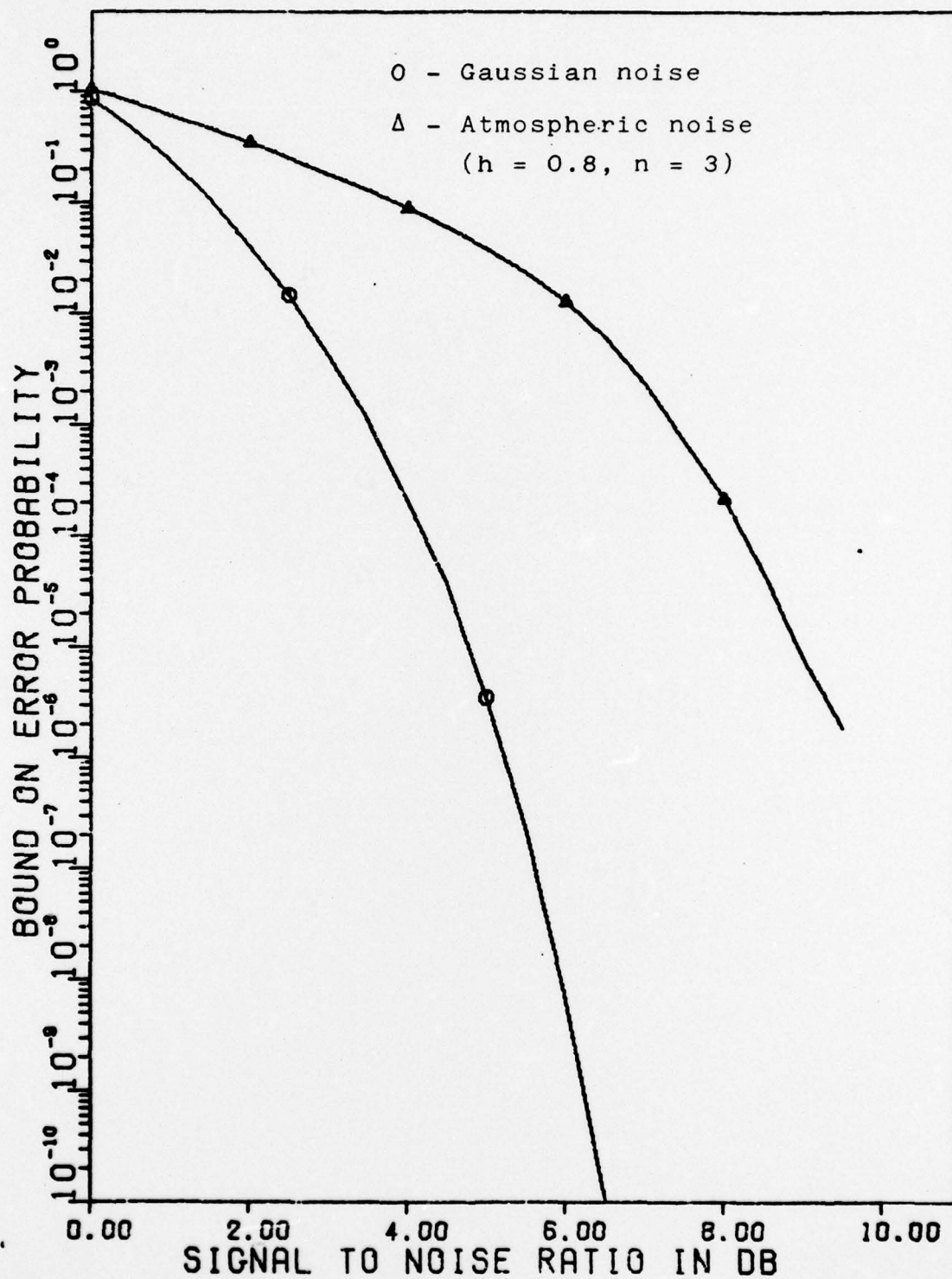


Figure 6. Probability of Symbol Error for Quaternary Coherent CPFSK,  $V_d = 4.0$ .

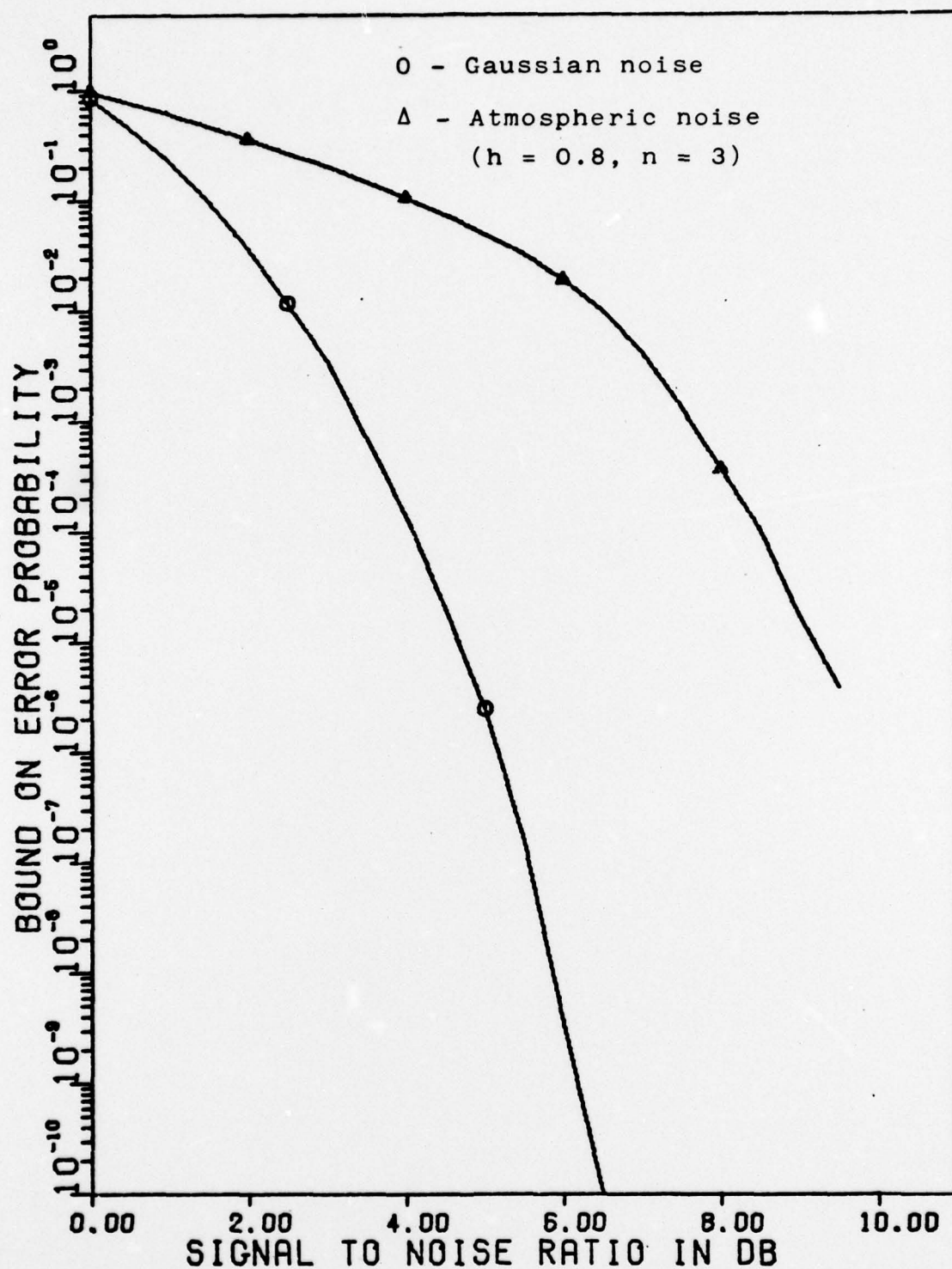


Figure 7. Probability of Symbol Error for Quaternary Coherent CPFSK,  $V_d = 5.0$ .

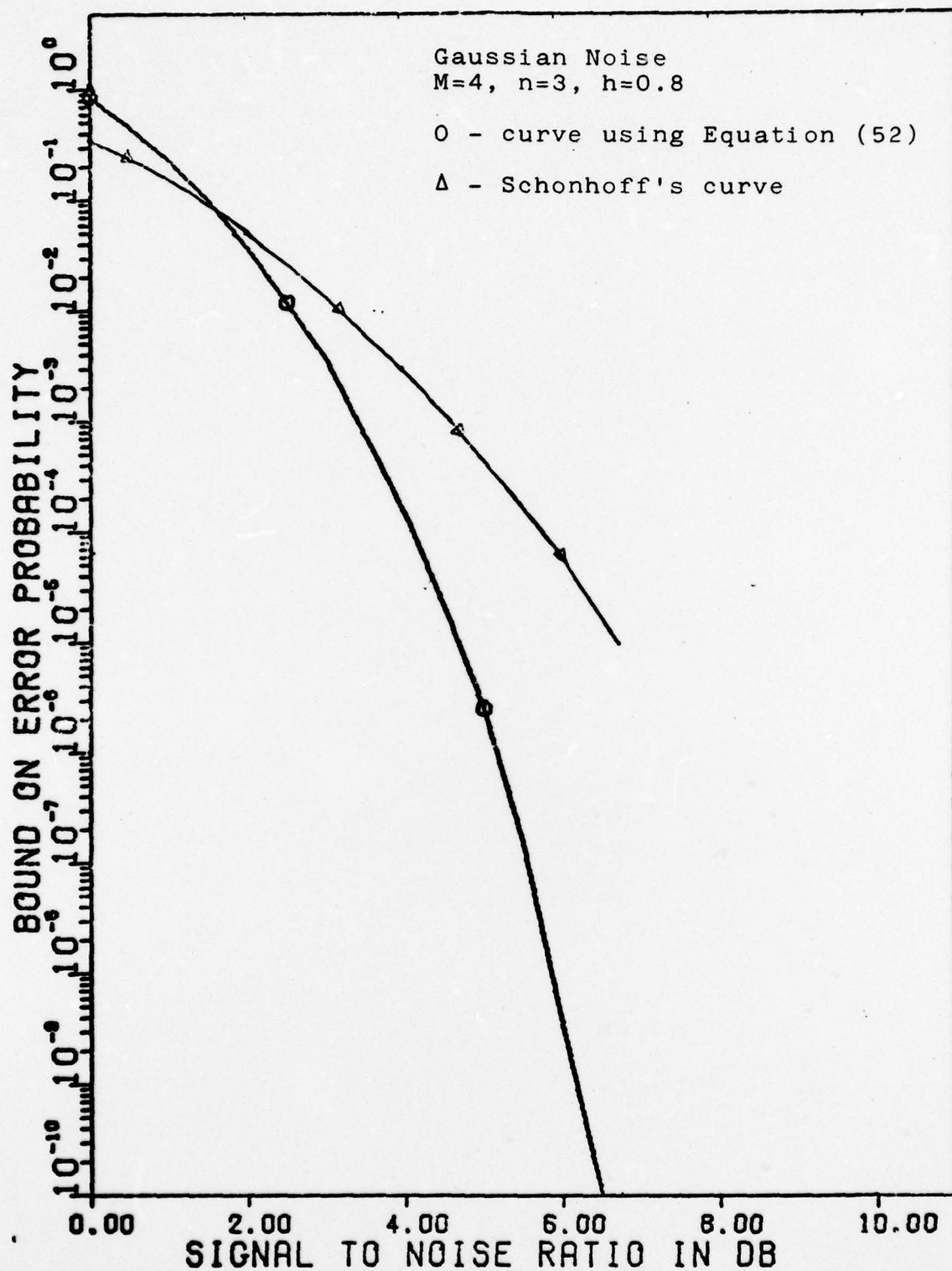


Figure 8. Probability of Symbol Error Comparison With Schonhoff's Results.



of error and for a SNR  $\geq 2.0$  he obtains a higher probability of error. The reason for this discrepancy could not be determined because Schonhoff's curves could not be reproduced using his equations (10) and (11) (Ref 4:346). The problem of reproducing Schonhoff's curves may be due to the evaluation of the error function. Schonhoff does not define the error function used in his report, and it is assumed he meant the usual definition:

$$\text{erf}(x) = (2/\pi)^{1/2} \int_0^x \exp [-u^2] du \quad (53)$$

If he used some other definition (i.e. Equation (65) in reference 14:37), this might account for the discrepancy. The discrepancy may also exist if Schonhoff has made a mistake in determining the number of correlations that need to be computed. Since some sequences of symbols have the same correlation, Schonhoff says he calculated only those with different correlations (Ref 4:647).



## V. Conclusions and Recommendations

Conclusions and recommendations cover two separate areas: the atmospheric noise model and the coherent M-ary CPFSK receiver performance.

### Atmospheric Noise Model

The Rayleigh-lognormal, mixed distribution model closely represents the Crichlow APD model of atmospheric noise if the correct parameter values for A and s are found for each particular  $V_d$  ratio. The present difficulty in using this model is the trial and error method used to obtain the correct parameters for various  $V_d$  ratios.

Further research should be done to identify a relationship between the  $V_d$  ratio and the parameters A and s so a parameter set could be easily found for any  $V_d$  ratio. Research also needs to be continued to find an atmospheric noise distribution model which has a closed form solution.

### Coherent M-ary CPFSK Receiver Performance

As seen in Figure 6 and Figure 7, the probability of error for this receiver is always greater when operating in an atmospheric noise environment. Wilson's evaluation of phase shift keying indicated that at low SNR, a PSK receiver may perform better in atmospheric

noise than in Gaussian noise (Ref 3:100-105).

Although results in this report do not fully justify the same conclusion, it still may be true. Performance results of a M-ary CPFSK receiver at low SNR may resemble Wilson's results if a performance bound for SNR is developed.

There are many areas that require further research in evaluating M-ary CPFSK receiver performance.

Five major areas are:

1. Need to obtain a performance bound for low SNR.
2. Need to evaluate receiver performance for different values of M and n.
3. Need to find the optimum value of h (deviation ratio) for different values of M and n in M-ary CPFSK when the interference is atmospheric noise.
4. Need to analyze the performance of a non-coherent M-ary CPFSK receiver.
5. Need to develop optimum coherent and noncoherent M-ary CPFSK receiver for atmospheric noise.

### Bibliography

1. Gamble, J. T. "An Analysis of Linear and Non-Linear Coherent Detection in Atmospheric Noise at Very Low Frequency." RADC Technical Report 74-289. Griffiss Air Force Base, New York: Rome Air Development Center, 1974.
2. Crichlow, W. Q., et al. "Determination of the Amplitude-Probability Distribution of Atmospheric Radio Noise from Statistical Moments." Journal of Research, National Bureau of Standards - D: Radio Propagation, 64D: 49-56 (1950)
3. Wilson, K. E. Analysis of the Crichlow Graphical Model of Atmospheric Radio Noise at Very Low Frequencies. M. S. Thesis, Wright-Patterson Air Force Base, Ohio: Air Force Institute of Technology, November 1974.
4. Schonhoff, T. A. "Symbol Error Probabilities for M-ary CPFSK: Coherent and Noncoherent Detection." IEEE Transactions on Communications Technology, Com-24: 644-652 (June, 1976)
5. Crichlow, William Q. "Noise Investigation at VLF by the National Bureau of Standards." Proceedings of the IRE, 45: 778-782 (June, 1957).
6. Spaulding, A. D., et al. "Conversion of the Amplitude-Probability Distribution Function for Atmospheric Radio Noise from one Bandwidth to Another." Journal of Research, National Bureau of Standards - D: Radio Propagation, 66D: 716-720 (1962).
7. Osborne, W. P. and M. B. Luntz. "Coherent and Non-coherent Detection of CPFSK." IEEE Transactions on Communications Technology, Com-22: 1023-1036 (August, 1974).
8. Beckmann, Petr. "Amplitude-Probability Distribution of Atmospheric Radio Noise," Journal of Research, National Bureau of Standards - D: Radio Science, 68D: 723-736 (1964).
9. Whalen, Anthony D. Detection of Signals in Noise. New York: Academic Press, Inc., 1971.
10. Beckmann, Petr. Probability in Communication Engineering. New York: Harcourt, Brace and World, 1967.



11. Davenport, W. B. Probability and Random Processes. New York: McGraw-Hill Book Co., 1970.
12. Meyer, Paul L. Introductory Probability and Statistical Applications. Reading, Mass.: Addison-Wesley Publishing Co., 1965.
13. National Bureau of Standards. Handbook of Mathematical Functions with Formulas, Graphs, and Mathematical Tables. Applied Mathematics Series-55, U. S. Department of Commerce., 1965.
14. Van Trees, Harry L. Detection, Estimation and Modulation Theory. Part 1. New York: John Wiley and Sons, 1968.



THIS PAGE IS BEST QUALITY PRACTICABLE  
FROM COPY FURNISHED TO DDC

THIS PAGE IS BEST QUALITY PRACTICABLE  
FROM COPY FURNISHED TO DDC

# Appendix A

The computer program used to evaluate the modified Bessel function of the first kind order zero is given below.

```
C      FIO=MODIFIED BESSEL FUNCTION OF FIRST KIND ORDER 0
      FUNCTION FIO(X)
      DIMENSION XL(6),XH(8)
      DOUBLE W
      DATA XL/3.5156229,3.0899424,1.2067492,0.2659732,0.0360768,
10     10.0045813/,XH/0.01328592,0.00225319,-0.00157565,0.00916281,
20     2-0.02057706,0.02635537,-0.01647633,0.00392377/
      W=X
      XA=ABS(X)
      IF (XA.GT.0.001) GO TO 10
      FIO=1.0
      RETURN
10     IF (X.GT.0) GO TO 20
      X=XA
20     T=X/3.75
      IF (T.GT.1.0) GO TO 40
      FIO=1.0
      DO 30 J=1,6
      FIO=FIO+XL(J)*(T** (2*J))
30     CONTINUE
      RETURN
40     FIO=0.39894228
      TI=1.0/T
      DO 50 J=1,8
      FIO=FIO+XH(J)*(TI**J)
50     CONTINUE
      FIO=FIO*DEXP(W)*(1.0/SQRT(X))
      RETURN
      END
```

### Vita

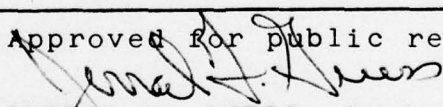
Kenneth Roger Olson was born on 9 January 1945 in Stewartville, Minnesota. He graduated from high school in Chatfield, Minnesota in 1963 and attended Mankato State College from which he received a Bachelor of Arts degree in June 1967. He began training at the Air Force Officer Training School in November 1967 and received his commission in February 1968. After spending nine months in Communications School at Keesler AFB, Mississippi, he was placed in charge of the technical control branch of the AUTODIN switching facility at Gentile AFS, Ohio. From August 1970 to September 1971 he served as shift supervisor at the AUTODIN switching center at Wildwood AFS, Alaska. He was then transferred to the 1931st Communications Group at Elmendorf AFB, Alaska where he served as Chief of Maintenance Staff until entering the School of Engineering, Air Force Institute of Technology, in June 1975.

Permanent address: Route 1

Chatfield, Minnesota 55923

UNCLASSIFIED

SECURITY CLASSIFICATION OF THIS PAGE (When Data Entered)

REPORT DOCUMENTATION PAGE		READ INSTRUCTIONS BEFORE COMPLETING FORM
1. REPORT NUMBER AFIT/GE/EE/77-33	2. GOVT ACCESSION NO.	3. RECIPIENT'S CATALOG NUMBER
4. TITLE (and Subtitle) PERFORMANCE ANALYSIS OF CONTINUOUS- PHASE FREQUENCY SHIFT KEYING MODULA- TION IN ATMOSPHERIC NOISE		5. TYPE OF REPORT & PERIOD COVERED MS Thesis
		6. PERFORMING ORG. REPORT NUMBER
7. AUTHOR(s) Kenneth R. Olson Captain, USAF		8. CONTRACT OR GRANT NUMBER(s)
9. PERFORMING ORGANIZATION NAME AND ADDRESS Air Force Institute of Technology (AFIT/EN) Wright-Patterson AFB, Ohio 45433		10. PROGRAM ELEMENT, PROJECT, TASK AREA & WORK UNIT NUMBERS
11. CONTROLLING OFFICE NAME AND ADDRESS Rome Air Development Center/DCCL Griffiss AFB, NY 13441		12. REPORT DATE December 1977
		13. NUMBER OF PAGES 47
14. MONITORING AGENCY NAME & ADDRESS (if different from Controlling Office)		15. SECURITY CLASS. (of this report) Unclassified
		15a. DECLASSIFICATION/DOWNGRADING SCHEDULE
16. DISTRIBUTION STATEMENT (of this Report) Approved for public release; distribution unlimited		
17. DISTRIBUTION STATEMENT (of the abstract entered in Block 20, if different from Report)		
18. SUPPLEMENTARY NOTES Approved for public release; IAW AFR 190-17  JERRAL F. GUESS, Captain, USAF Director of Information		
19. KEY WORDS (Continue on reverse side if necessary and identify by block number) Frequency Modulation Atmospheric Noise Very Low Frequency Error Performance Prediction Noise Models		
20. ABSTRACT (Continue on reverse side if necessary and identify by block number) Continuous phase frequency shift keying (CPFSK) is potentially an attractive modulation scheme with performance better than PSK in Gaussian noise. The optimum coherent M-ary CPFSK receiver has been developed for operation in Gaussian noise. In this report the optimum receiver performance is evaluated assuming operation at very low frequencies.		



UNCLASSIFIED

SECURITY CLASSIFICATION OF THIS PAGE(When Data Entered)

Atmospheric noise is the most prevalent interference when operating at very low frequencies. An analytic amplitude probability distribution (APD) function is developed that closely approximates the Crichlow atmospheric noise APD model which is based on empirically measured data. The analytic expression for the APD was developed by combining a Rayleigh and a lognormal density and obtaining the corresponding distribution function. By correctly choosing values for two parameters in the distribution, it approximates the atmospheric noise APD for various  $V_d$  ratios.

The performance of the optimum coherent M-ary CPFSK receiver was evaluated for  $M=4$  and  $n=3$  operating in atmospheric noise with specific  $V_d$  ratios (4 & 5). The evaluation consists of finding a probability of error bound for a sub-optimum receiver, which is valid for high signal-to-noise ratios (SNR). Results indicate that the receiver performance in atmospheric noise becomes increasingly worse compared to Gaussian noise as the SNR increases.

UNCLASSIFIED

SECURITY CLASSIFICATION OF THIS PAGE(When Data Entered)